J. Electroanal. Chem., 115 (1980) 211—224

ELECTROCHEMICAL FORMATION AND REDUCTION OF SILVER OXIDES IN ALKALINE MEDIA

JOHN M.M. DROOG and FRED HUISMAN

Van 't Hoff Laboratory, State University of Utrecht, Padualaan 8, Utrecht (The Netherlands)

(Received 2nd July 1980)

ABSTRACT

The anodic oxidation of silver electrodes in NaOH solution and the reduction of the silver oxides formed were studied by potential step chronoamperometry. Oxidation of Ag to Ag_2O is a diffusion-controlled reaction, the diffusion control being established in the solid phase. Oxidation of Ag_2O to AgO proceeds via a nucleation and growth-controlled process. The amount of AgO decreased with increasing step height. The current—time curves for this reaction have been analysed with the Kolmogoroff—Avrami equation. Reduction of AgO to Ag_2O occurs initially on the outside of the electrode, and the rate of the reaction is limited by diffusion of ions across the thickening layer of Ag_2O. Reduction of Ag_2O to Ag proceeds via a nucleation and growth reaction.

INTRODUCTION

In 1908 Luther and Pokorny [1] reported on their study of the electrochemical behaviour of silver and its oxides. They realized that this study had technological importance because silver oxides were used as positive electrodes in alkaline accumulators. Since that time a large number of investigations have been published concerning the silver electrode in alkaline electrolyte and many reviews have been written [2—15].

Galvanostatic measurements

Most investigators used the galvanostatic technique. This method involves subjecting the electrode to a constant current and measuring its potential as a function of time. The potential shifts rapidly due to charging of the double layer. This shift continues until a potential is reached where a faradaic process can occur and the charge can be accepted without further change in the electrode potential. Figure 1 shows a typical galvanostatic charging curve for silver in NaOH [16—45]. The portion up to point B shows the anodic charging curve and the portion after point B the cathodic charging curve.

From simultaneous X-ray diffraction studies, Wales and Burbank [29] concluded that Ag_2O was formed during the first plateau (1), and AgO during the second. This is in agreement with other studies using X-ray analysis [24,34,39], electron diffraction [23,36,37] and chemical analysis [38]. AgO patterns were

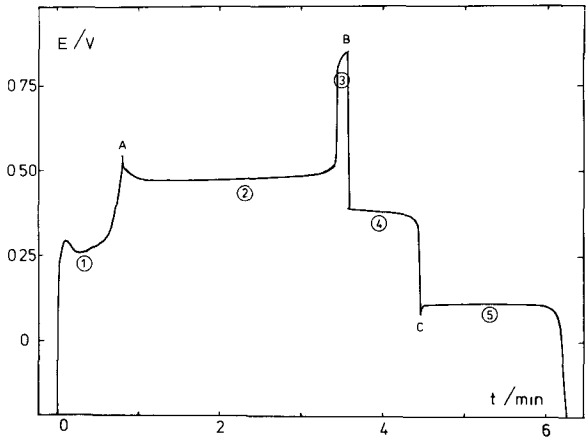

Fig. 1. Galvanostatic oxidation of reformed Ag in 1 mol dm^{-3} NaOH at 0.95 mA and 22°C followed by galvanostatic reduction at −1.05 mA. Apparent surface area 0.2 cm^2.

found shortly after the beginning of plateau 2, which was taken to indicate that AgO forms initially at the outside of the Ag_2O layer [29,34]. This is supported by the results of Ross and Roberts [44], who showed that light is able to assist the conversion of Ag_2O to AgO and that the effect of light decreases as the AgO film thickens and less light can penetrate to the AgO/Ag_2O interface. Oxygen is evolved during the potential plateau 3.

The second plateau is preceded by a small peak (A). Several explanations have been proposed for its occurrence. Hickling and Taylor [17] ascribed it to the formation of an oxide higher than AgO which decomposes to give the latter substance. Jones et al. [18] suggested that the peak is associated with the fact that AgO nuclei do not form easily in the Ag_2O layer. Dirkse [19] suggested that the peak is due to a maximum ohmic potential drop associated with a complete film of Ag_2O. Cahan et al. [22] concluded from measurements of the resistance of the Ag_2O layer that the peak is not directly due to an ohmic resistance effect but to concentration of the current in small localized areas, where the conversion of Ag_2O to AgO can proceed. Yoshizawa and Takehara [24] believed that the peak is generated because O^{2-} ions can diffuse more easily in the AgO layer than in the Ag_2O layer. Gossner et al. [36,37] revived the old explanation of Hickling and Taylor by stating that the peak in the galvanostatic charging curve is closely related to the formation of "AgO_x" (which they discovered with electron diffraction). However, this oxide has not been found by other investigators [23,29].

On discharge, AgO is reduced to Ag_2O during plateau 4. Chemical analysis [38] showed that there is no change in the amount of silver ion in the film. Ag_2O forms initially on the surface of the AgO, as was indicated by its early appearance in the X-ray diffraction patterns [29]. Transition from plateau 4 to plateau 5 occurs before complete reduction of AgO to Ag_2O [29,38]. At plateau 5 both AgO and Ag_2O are being discharged simultaneously and the layer of Ag_2O always covers the AgO [7,9,29]. A voltage peak (C) is observed [9,10,24] between plateau 4 and plateau 5.

In the charging situation, the Ag/Ag_2O plateau does not persist as long as the

Ag_2O/AgO level, especially at higher current density [24,32,34,35,41,43]. This has led to the conclusion that the layer of AgO is thicker than that of Ag_2O [2,3,4,7]. On the other hand, it is also possible that the $Ag \rightarrow Ag_2O$ reaction continues to occur alongside the $Ag_2O \rightarrow AgO$ reaction [20].

In contrast to the charging situation, the AgO/Ag_2O plateau in the discharging curve is shorter than the Ag_2O/AgO plateau. The length of the AgO/Ag_2O plateau decreases if the current density is increased [7,13,24].

A coulombic efficiency of 100% has been reported [20,24], i.e. the total amount of electricity during charging is equal to the total amount of electricity during discharging. From Fig. 1 it is clear that the power efficiency is lower, since most of the charging occurs at the Ag_2O/AgO level, and most of the discharging at the Ag/Ag_2O level.

Potentiodynamic measurements

Dirkse and De Vries [46] and Croft [47] were the first to apply a continuously varying potential to the silver electrode and measure the resulting current. This potentiodynamic technique enables us to obtain a quick "electrochemical spectrum" of a system, and it has been widely used in studying the silver electrode/alkaline electrolyte interface [38,46—68]. Being, in effect, a differential method it sometimes has advantages over the galvanostatic method for the detection of various stages of oxidation and reduction of electrode surfaces.

Cyclic voltammograms for the silver/alkaline solution system generally show four oxidation peaks in the anodic sweep and two reduction peaks in the cathodic sweep [59,60,67] (see Fig. 2). During the cathodic sweep a "secondary" anodic peak is sometimes observed before the first reduction peak appears [51,65]. There is general agreement in the literature that the two major anodic peaks are related to the formation of Ag_2O and AgO and that the cathodic peaks can be assigned to the reduction of AgO and Ag_2O. A peak before the main Ag_2O formation peak has been variously attributed to the formation of

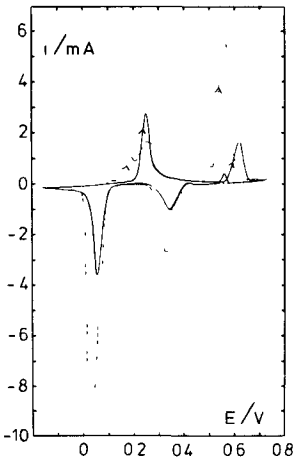

Fig. 2. Triangular sweep voltammogram for polished (———) and reformed (- - - - - -) silver in 1 mol dm^{-3} NaOH, 22°C. Potential sweep rate = 20 mV s^{-1}.

AgOH [46,50], to preferential oxidation of an activated lattice [55,63] and to the dissolution of silver as $Ag(OH)_2^-$ with diffusion of the product into the solution [59,60]. Sensitive measurements combined with ellipsometry [67,68] showed that before that stage there is electrosorption of monolayer amounts of oxygen, together with the dissolution of silver species. A large difference in the reactivity of the Ag(111) and the Ag(110) crystal face was observed [68].

During a complete cycle the total oxidation and reduction charges are identical [51,52,57,66], demonstrating that practically all the oxidation products remain on the electrode. The amount of electricity used to form AgO is considerably less than the amount used to form Ag_2O [48,51,52,64,66]. The conversion of Ag_2O to AgO decreased with increasing sweep rate [48,64].

The peak current for the Ag_2O formation is proportional to the square root of the sweep rate [38,55,59,64]. The peak current does not depend on whether or not the solution is stirred [38,59], nor on the rotation speed of the electrode [59,63], nor on the OH^- concentration [55]. This indicates that the rate of Ag_2O formation is controlled by a diffusion process in the oxide phase [38,55].

For the formation of AgO from Ag_2O [51], as well as for the reduction of Ag_2O to Ag [59], an autocatalytic effect has been reported, e.g. upon reversing the potential sweep before the current has reached its peak value, a characteristic continuing increase of current is observed. This means that the processes corresponding to these peaks are controlled by nucleation and growth.

Potential step chronoamperometry measurements

In the case of nucleation and growth-controlled processes, experimental studies using the potential step chronoamperometry method are usually to be preferred, because then the electrochemical rate parameters are constant for $t > 0$.

In view of the large number of investigations concerning the anodic oxidation of silver in alkaline solution, it is remarkable that only a few systematic potential step chronoamperometry studies have been reported.

Vidovich et al. [69] and Oshe [70] studied the conversion of Ag to Ag_2O. Fleischmann et al. [71,72] reported on the reactions $Ag \rightarrow Ag_2O$, $Ag_2O \rightarrow AgO$ and $Ag_2O \rightarrow Ag$. Lyamina et al. [73] investigated the reduction of Ag_2O to Ag. Gossner et al. [36,37] studied oxidation reactions starting from silver.

In this paper we report on our potential step chronoamperometry studies relating to the oxidation of silver and the reduction of silver oxides. The results are compared with the results of galvanostatic and potentiodynamic measurements.

EXPERIMENTAL

Silver discs (diam. 5 mm, thickness 3—4 mm) cut from a polycrystalline rod (Drijfhout, 99.999% pure) were used as working electrodes. The discs were sealed into acrylic resin (Technovite 4071) in such a way that only the top surface of the metal was exposed to the solution. The electrode surfaces were

mechanically polished; in the last stage with diamond pastes containing particles of 0.25 μm. Before the electrochemical measurements the electrodes were reduced cathodically.

The reference electrode was an Ingold "Argenthal" electrode (Ag/AgCl|KCl-(3*M*); E = 207 mV vs. NHE), separated from the main compartment.

The potential difference between working electrode and reference electrode was controlled by a Wenking LB 75L potentiostat that was programmed with a Wenking VSG 72 voltage scan generator.

For scanning electron microscopy the samples were cut from the resin, briefly cleaned in twice-distilled water and allowed to dry in air. The samples were mounted on aluminium tables. By Courtesy of Prof. J.W. Geus, scanning electron microscopy was performed in a Cambridge Stereoscan 150.

RESULTS

Polished and reformed electrodes

Like most of the other workers in the field of anodic oxidation of silver, we did the majority of measurements on reformed electrodes, i.e. electrodes that had been subjected to several oxidation—reduction cycles.

There is a difference in the electrochemical behaviour of freshly polished electrodes and reformed electrodes. This is illustrated in Fig. 2 which shows a potentiodynamic charging curve for each type of electrode. The two curves clearly differ, both with respect to the form of the peaks and to the amount of charge connected with them.

Oxidation—reduction cycles greatly change the state of the silver surface; this is best illustrated by the SEM pictures in Fig. 3. The smooth surface has been changed into a reformed silver surface composed of nodular deposits.

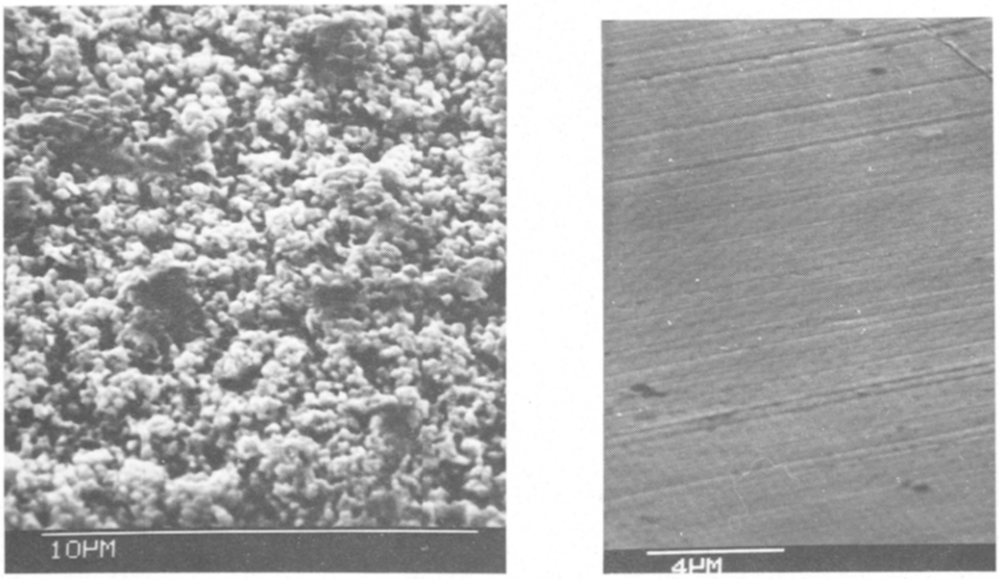

Fig. 3. Scanning electron micrographs of polished (right) and reformed (left) silver surfaces.

We determined the surface area using a method proposed by Vashkyalis and Demontaite [74]: the amount of charge connected with the underpotential deposition of lead from a 1 mol dm^{-3} NaOH solution containing 5×10^{-4} mol dm^{-3} $Pb(NO_3)_2$ is measured. Using this method we found the surface area of the reformed silver surface to be about four times larger than that of the smooth surface.

The optical parameters for the reformed surface as measured by ellipsometry (n = 1.8, k = 1.8 at λ = 632.8 nm) are very different from those for the smooth surface (n = 0.2, k = 3.8). In addition, the reformed surfaces showed a greatly increased off-specular scattering of light.

Oxidation at constant potential

Oxidation starting from Ag

Chronoamperometry curves for reformed silver surfaces were measured with −200 mV as starting potential and step potentials in the +200 mV to +800 mV region. After 2 min the oxidation products were reduced potentiodynamically at a sweep rate of 20 mV s^{-1}, and the concomitant stripping voltammogram was recorded to obtain an electroanalysis of the silver oxide layer.

Three characteristic regions of step potential can be distinguished and typical examples are given in Figs. 4—6.

For step potentials in the 200—500 mV region, curves are obtained which show a marked fall in the current immediately after the positive potential is imposed on the electrode (Fig. 4a). The corresponding stripping voltammogram shows only a peak for the reduction of Ag_2O (Fig. 4b). The charges under the current—time curves and under the stripping curves are about 20 mC. (The geometrical surface area of the electrodes is 0.2 cm^2.)

For step potential in the 500—700 mV region, the current, after falling initially, rises again, reaches a maximum value and finally falls again (Fig. 5a). The current—time curves are strongly dependent on the value of the step potential. For higher potentials the current peak is higher and appears at a shorter oxidation time. In the stripping voltammogram (Fig. 5b) two peaks appear: one for the reduction of AgO and one for the reduction of Ag_2O.

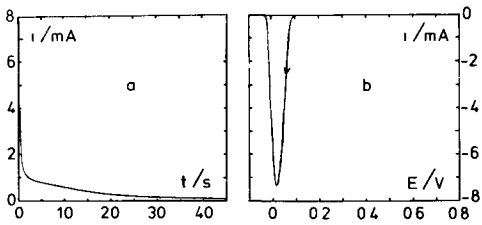

Fig. 4. (a) Current—time curve after a potential step from −200 mV to +460 mV for reformed silver in 1 mol dm^{-3} NaOH. (b) Subsequent stripping voltammogram at a sweep rate s = 20 mV s^{-1}.

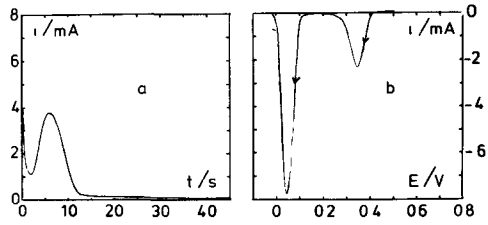

Fig. 5. (a) Current—time curve after a potential step from −200 mV to +510 mV for reformed silver in 1 mol dm^{-3} NaOH. (b) Subsequent stripping voltammogram at s = 20 mV s^{-1}.

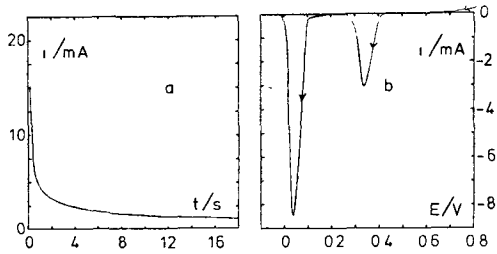

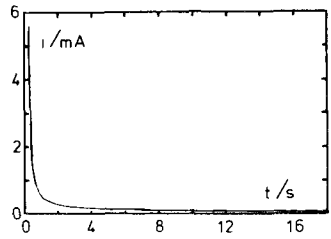

Fig. 6. (a) Current—time curve after a potential step from −200 mV to +810 mV for reformed silver in 1 mol dm^{-3} NaOH. (b) Subsequent stripping voltammogram at s = 20 mV s^{-1}.

Fig. 7. Current—time curve after a potential step from −200 mV to +400 mV for polished silver in 1 mol dm^{-3} NaOH.

For step potentials above 700 mV (Fig. 6a) the current peak occurs after such a short time that it can no longer be resolved. In this case the current does not reach zero and oxygen evolution can be visually observed at the electrode surface. The stripping voltammogram (Fig. 6b) shows peaks for AgO and Ag_2O.

Chronoamperometry curves for polished silver electrodes showed the same trends as those for the reformed surfaces. There is, however, one remarkable difference; for polished surfaces the curves for 200 mV $< E_{step} <$ 500 mV are exponentially falling curves (Fig. 7), without the inclination observed for reformed electrodes (Fig. 4a).

Oxidation starting from Ag_2O

Electrodes on which Ag_2O had been formed during 2 min of polarization at 400 mV were investigated further by chronoamperometry with potential steps into the 500—700 mV region (Fig. 8a). The current—time curves obtained display the same characteristics. The current has an initial zero value, increases to a maximum and then decreases to zero again. If the final potential is chosen more anodic, less time is required to reach the maximum. Charge—time curves were obtained by planimetric integration. The total amount of electricity connected with the AgO formation decreased with increasing step potential (Fig. 9).

Stripping voltammograms (Fig. 8b) showed that the compound formed during anodisation is AgO. The AgO reduction peak was smaller for electrodes that were anodized at higher potentials.

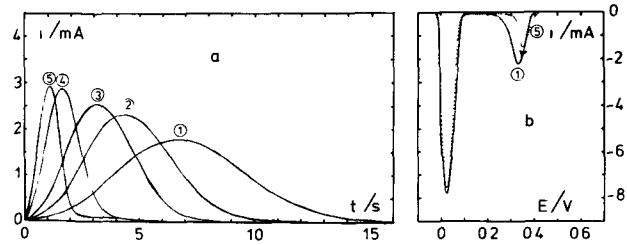

Fig. 8. (a) Current-time curves after potential steps from 400 mV to (1) 530, (2) 550, (3) 575, (4) 600, (5) 635 mV. (b) Subsequent stripping voltammograms at s = 20 mV s^{-1}.

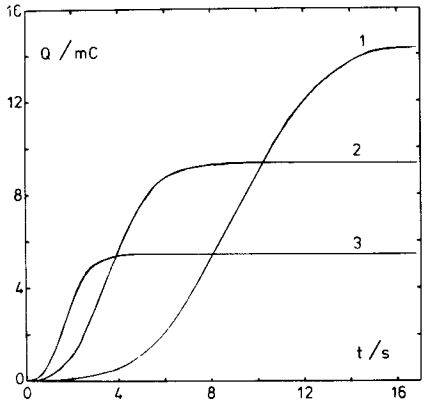

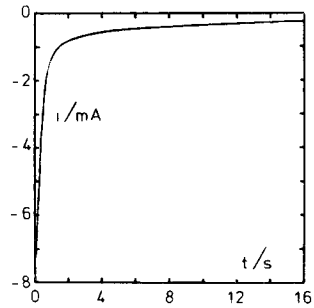

Fig. 9. Charge vs. time curves after potential steps from 400 mV to: (1) 515, (2) 565, (3) 600 mV.

Fig. 10. Current—time curve after a potential step from 700 to 200 mV.

Reduction at constant potential

Reduction starting from AgO

Silver electrodes were oxidized by an anodic potential scan (dE/dt = 20 mV s^{-1}) up to 700 mV and the scan was arrested at that potential for 1 min. Then the electrode potential was stepped to lower values and chronoamperometry curves were recorded.

Two characteristic regions of step potential can be distinguished. Typical examples are given in Figs. 10 and 11.

For step potentials above 100 mV the curves initially show a high reduction current, but this falls rapidly to low values (Fig. 10).

For step potentials below 100 mV, the reduction current, after falling initially, rises again, reaches a maximum value and finally falls again (Fig. 11). The

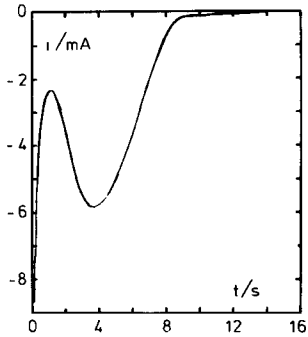

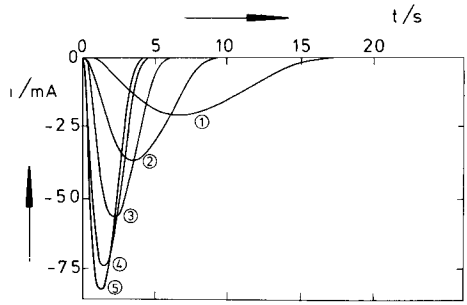

Fig. 11. Current—time curve after a potential step from 700 to 50 mV.

Fig. 12. Current—time curves after potential steps from 400 mV to. (1) 80, (2) 70, (3) 40, (4) 25, (5) 10 mV.

step potential was observed to have a strong influence. For lower potentials the current peak is higher and appears at a shorter reduction time.

Reduction starting from Ag_2O

Ag_2O-covered electrodes, formed by anodic polarization at 400 mV for 2 min, were reduced at constant potentials in the +100 mV to −300 mV region. Examples of the current—time curves obtained are given in Fig. 12. In all curves the (negative) current first rises, then reaches a maximum and finally becomes zero again. As the potential becomes more cathodic the current peak increases and occurs at a shorter reduction time.

DISCUSSION

Oxidation

Curves like the curve shown in Fig. 5a have also been reported by Gossner et al. [36,37]. Their statement that the current peak can be attributed to the reaction $Ag \rightarrow Ag_2O$ must be wrong, since the appearance of the current peak in the chronoamperogram leads to an AgO peak being present in the stripping voltammogram (Fig. 5b). It is obvious from Figs. 4—8 that two processes are to be considered, e.g. oxidation of Ag to Ag_2O (Fig. 4a) and oxidation of Ag_2O to AgO (Fig. 8a) and that the curve in Fig. 5a is due to these two reactions occurring simultaneously.

Above 700 mV the oxygen evolution reaction comes into play (Fig. 6a).

The reaction $Ag \rightarrow Ag_2O$

Figure 7 shows potentiostatic formation of Ag_2O on polished electrodes. The current transients are monotonically falling curves [36,70,71]. The curves have the form predicted for diffusion-controlled processes [70]. The diffusion control is established by the reagent travelling in the solid phase, and the diffusion layer becomes thicker as the oxide layer grows.

On reformed electrodes the curves are somewhat different (Fig. 4a) and resemble those reported by Vidovich et al. [69]. These curves show the complexity of diffusion on distorted surfaces such as those shown in the SEM picture in Fig. 3b.

From the amount of the charge associated with this process (20 mC), the geometric surface area of the electrode (0.2 cm^2) and the density of Ag_2O (7.143 g cm^{-3} [75]), we calculated the thickness of the oxide to be 170 nm.

The reaction $Ag_2O \rightarrow AgO$

The curves relating to this reaction (Fig. 8a) clearly show the characteristics of a nucleation and growth-controlled process. The amount of charge decreases with increasing potential (Fig. 9). It is always less than the charge consumed in the formation of Ag_2O, so it can be concluded that not all the Ag_2O is oxidized to AgO. Each charge—time plot (Fig. 9) can be described by the Kolmogoroff—Avrami equation [76—79]:

$$\alpha = 1 - \exp(-\alpha_{ext}) \quad (1)$$

where α is the fraction of volume occupied by the new phase and α_{ext} the fraction that would be occupied in the absence of overlap. α_{ext} is a function of time:

$$\alpha_{ext} = kt^n \quad (2)$$

where k is the rate constant, t the time and n a constant. In eqn. (2) the parameters k and n depend on the growth law of a single, growing centre and on the time dependence of the nuclei population [76—81].

Avrami and Kolmogoroff assumed that centres grow in all directions at a constant rate. This means that mass transport to the growing centres plays no role, which is a reasonable assumption in situations such as crystallization in supercooled liquids or supersaturated solutions. For three-dimensional growth, $n = 3$ if all nuclei are formed instantaneously, and $n = 4$ if nucleation centres are created at a constant rate (progressive nucleation).

Equation (1) can be linearized to [82]

$$\ln\{-\ln(1 - \alpha)\} = \ln k + n \ln t \quad (3)$$

With eqn. (3), n and k for the reaction $Ag_2O \rightarrow AgO$ can be calculated for the various potentials. A plot of ln k vs. E is shown in Fig. 13.

The parameter n was found to be about 2.5. We suggest that this value can be interpreted as follows: for the formation of AgO it is necessary that ions diffuse to the boundaries of the growing centres. Therefore, it is unrealistic to assume that the centres grow in all directions at a constant rate, i.e. that the dimensions of the centres increase proportional to time. It is much more likely that the dimensions grow approximately proportional to $t^{1/2}$. For three-dimensional growing centres this would lead to $n = 1.5$ for instantaneous nucleation and to $n = 2.5$ for progressive nucleation. Brownstein and Tarr [83] have used similar reasoning when discussing reordering of a nematic-cholesteric liquid crystal mixture.

Reduction

The reduction curve in Fig. 11 resembles the oxidation curve in Fig. 5a. From a comparison with Figs. 10 and 12 it can be concluded that this curve represents the simultaneous reduction of AgO to Ag_2O and of Ag_2O to Ag.

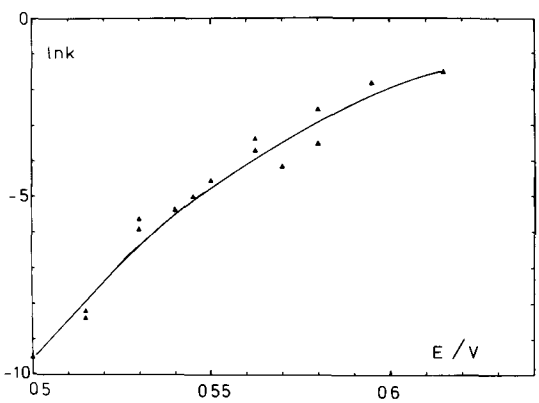

Fig. 13. Variation in ln k for the oxidation of Ag_2O to AgO with the electrode potential E.

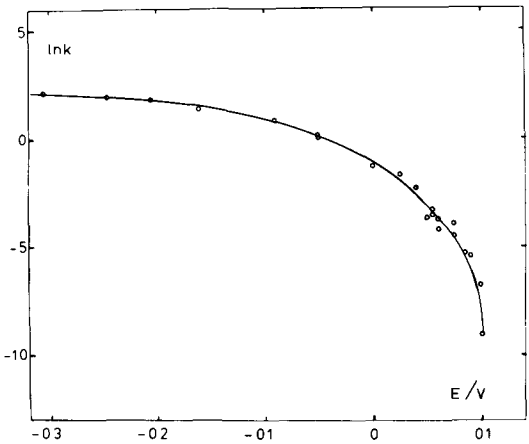

Fig. 14. Potential dependence of ln k for the reduction of Ag_2O to Ag.

The reaction $AgO \rightarrow Ag_2O$

During reduction of AgO, Ag_2O forms initially on the AgO electrolyte interface [29], and there is no change in the amount of silver ion in the oxide film [38].

The chronoamperometric curve in Fig. 10 has the form as predicted for diffusion-controlled processes [70]. The diffusion layer becomes thicker as the Ag_2O layer, which separates the AgO from the electrolyte, grows.

The reaction $Ag_2O \rightarrow Ag$

The curves relating to this reaction show the characteristics of a nucleation and growth-controlled process. The current transients were analysed by the Kolmogoroff—Avrami equation. The plot of ln k vs. the electrode potential is shown in Fig. 14. The value of n was found to be about 2.5, just as in the $Ag_2O \rightarrow AgO$ reaction.

Comparison of chronoamperometry results with galvanostatic and potentiodynamic results

When a silver electrode is charged at constant anodic current, the electrode potential rises until a potential is reached where the reaction $Ag \rightarrow Ag_2O$ can occur and the charge can be consumed by this faradaic process. As the Ag_2O layer grows thicker, the diffusion of ions across this layer becomes increasingly difficult, until the reaction rate is too slow to consume all the current that is forced through the electrode. The potential therefore rises to a value where AgO nuclei begin to be formed at the Ag_2O/electrolyte interface (peak A in Fig. 1). After nuclei have been formed, further growth of AgO is possible at a somewhat lower potential, and the reaction $Ag \rightarrow Ag_2O$ continues. After a certain time the reaction rate again cannot keep up with the controlled current, and the potential rises to oxygen evolution values.

During discharge at constant current, Ag_2O forms initially on the surface of the AgO (region 4 in Fig. 1) until diffusion limitation in the Ag_2O layer that

separates the AgO from the electrolyte prevents this reaction from keeping up with the imposed current and the potential is further lowered to a value where Ag_2O can be reduced to Ag. Since this last reaction requires a crystallization overpotential a potential peak is observed (peak C in Fig. 1).

With regard to potentiodynamic measurements, it is clear that the explanation of Clarke et al. [55] and Hampson et al. [63] about the origin of the "pre-Ag_2O" peak is the most plausible one, i.e. that the complexity of the Ag_2O peak in the voltammogram is associated with the heavy disorder of the silver surface. Another feature that can be explained is that the conversion of Ag_2O to AgO decreases with increasing sweep rate [48,64]. At high sweep rates most of the AgO is formed at higher potentials than in the case of low sweep rates, and so less AgO is formed (see Fig. 9).

CONCLUSION

Chronoamperometry is a useful technique for studying phase formation on electrodes.

Anodic oxidation of silver is a complex reaction and the measurements depend strongly on the pretreatment of the electrode surface. The main oxidation reactions are $Ag \rightarrow Ag_2O$, $Ag_2O \rightarrow AgO$, and evolution of oxygen. The rate of the reaction $Ag \rightarrow Ag_2O$ is limited by the diffusion of ions across the thickening oxide layer. Further oxidation to AgO proceeds via a nucleation and growth-controlled process.

The reduction rate of AgO to Ag_2O is limited by the diffusion of ions across the Ag_2O layer that separates the AgO from the electrolyte. Conversion of Ag_2O to Ag proceeds via a nucleation and growth-controlled process.

The nucleation and growth processes have been analysed with the Kolmogoroff—Avrami equation. For the reduction of Ag_2O to Ag, the growth laws for the growing centres show a $t^{2.5}$ time dependence. This can be explained by three-dimensional growth with progressive nucleation, with the dimensions of the centres growing proportional to $t^{1/2}$ (diffusion behaviour).

REFERENCES

1 R. Luther and F. Pokorny, Z. Anorg. Allg. Chem., 57 (1908) 290.
2 T.P. Dirkse, J. Electrochem. Soc., 106 (1959) 453.
3 L. Young, Anodic Oxide Films, Academic Press, London, 1961, p. 302.
4 J.A. MacMillan, Chem. Rev., 62 (1962) 65.
5 J.A. Allen, Proc. 1st Australian Conference on Electrochemistry, Pergamon Press, Oxford, 1965, p. 76.
6 C. Vanleugenhaghe, M. Pourbaix and P. Van Rysselberghe, in M. Pourbaix (Ed.), Atlas of Electrochemical Equilibria in Aqueous Solutions, Pergamon Press, London, 1966, p. 393.
7 J.P. Hoare, The Electrochemistry of Oxygen, Interscience, New York, 1968, p. 211.
8 L.M. Gedansky and L.G. Hepler, Engelhard Ind. Tech. Bull., 9 (1969) 117.
9 G.N. Nagy and E.J. Casey in A. Fleischer and J.J. Lander (Eds), Zinc—Silver Oxide Batteries, Wiley, New York, 1971, p. 133.
10 H.R. Thirsk and D. Lax in A. Fleischer and J.J. Lander (Eds.), Zinc—Silver Oxide Batteries, Wiley, New York, 1971, p. 153.
11 N.A. Hampson, J.B. Lee and J.R. Morley, Electrochim. Acta, 16 (1971) 637.
12 Gmelins Handbuch der Anorganische Chemie, Part B1, 8th ed., 1971, p. 125.
13 S. Toshima, Progr. Surf. Membr. Sci., 4 (1971) 231.
14 Gmelins Handbuch der Anorganische Chemie, Part A4, 8th ed., 1974, pp. 243—279.

15 N.A. Shumilova and G.V. Zhutaeva, in A.J. Bard (Ed.), Encyclopedia of Electrochemistry of the Elements, Vol. VIII, Marcel Dekker, New York, 1978, p. 1.
16 J.A. Denison, Trans. Electrochem. Soc., 90 (1946) 387.
17 A. Hickling and D. Taylor, Discuss. Faraday Soc., 1 (1947) 277.
18 P. Jones, H.R. Thirsk and W.F.K. Wynne-Jones, Trans, Faraday Soc., 52 (1956) 1003.
19 T.P. Dirkse, J. Electrochem. Soc., 106 (1959) 920.
20 G.L. Vidovich, D.I. Leikis and B.N. Kabonov, Dokl. Akad. Nauk S.S.S.R., 124 (1959) 125.
21 C.P. Wales and J. Burbank, J. Electrochem. Soc., 106 (1959) 885.
22 B.D. Cahan, J.B. Ockerman, R.F. Amlie and P. Rüetschi, J. Electrochem. Soc., 107 (1960) 725.
23 G. Poli, Z. Siedlecka and B. Rivolta, Inst. Lomb. (Rend. Sci.), 97 (1963) 631.
24 S. Yoshizawa and Z. Takehara, J. Electrochem. Soc. Jap., 31 (1963) 91.
25 R. Piontelli, L. Peraldo Bicelli and C. Romagnani, Lincei-Rend. Sci. Fis. Mat. Nat., 36 (1964) 18.
26 R.G. Barradas and G.H. Fraser, Can. J. Chem., 42 (1964) 2488.
27 E.J. Casey and W.J. Moroz, Can. J. Chem., 43 (1965) 1199.
28 Yu.S. Gorodetskii, Sov. Electrochem., 1 (1965) 600.
29 C.P. Wales and J. Burbank, J. Electrochem. Soc., 112 (1965) 13.
30 T.P. Dirkse, Electrochem. Technol., 4 (1966) 163.
31 T.P. Dirkse, D. De Wit and R. Shoemaker, J. Electrochem. Soc., 114 (1967) 1196.
32 A. Langer and J.T. Patton, J. Electrochem. Soc., 114 (1967) 113.
33 Z. Takehara, Y. Namba and S. Yoshizawa, Electrochim. Acta, 13 (1968) 1395.
34 G.D. Briggs, M. Fleischmann, D.J. Lax and H.R. Thirsk, Trans. Faraday Soc., 64 (1968) 3120.
35 M.J. Dignam, H.M. Barrett and G.D. Nagy, Can. J. Chem., 47 (1969) 4253.
36 K. Gossner, Th. Eftychiadis and D. Körner, Z. Naturforsch., 24a (1969) 807.
37 K. Gossner, Th. Eftychiadis and D. Körner, Z. Naturforsch., 24a (1969) 813.
38 N. Sato and Y. Shimizu, Electrochim. Acta, 18 (1973) 567.
39 H. Franssen, E. Häusler and W. Böhnstedt, Metalloberflache Angew. Elektrochemie, 28 (1974) 140.
40 R.S. Perkins and M.L. Woods, J. Electroanal. Chem., 32 (1974) 151.
41 C.P. Wales, J. Electrochem. Soc., 121 (1974) 17.
42 C.P. Wales, J. Electrochem. Soc., 121 (1974) 727.
43 D.B. Gibbs, B. Rao, R.A. Griffin and M.J. Dignam, J. Electrochem. Soc., 122 (1975) 1167.
44 D. Ross and E.F.I. Roberts, Electrochim. Acta, 21 (1976) 371.
45 S. Lică, Rev. Roum. Chim., 29 (1978) 837.
46 T.P. Dirkse and D.B. De Vries, J. Phys. Chem., 63 (1959) 107.
47 G.T. Croft, J. Electrochem. Soc., 106 (1959) 278.
48 M.R. Tarasevich, N.A. Shumilova and R.K. Burshstein, Izv. Akad. Nauk. S.S.S.R., 1 (1964) 14.
49 D.H. McClelland and M. Shaw, Ext. Abstr., The Electrochem. Soc., Battery Division, Vol. 10, 1965, p. 32.
50 P. Stonehart, Electrochim. Acta, 13 (1968) 1789.
51 P. Stonehart and F.P. Portante, Electrochim. Acta, 13 (1968) 1805.
52 H. Göhr and A. Breitenstein, Electrochim. Acta, 13 (1968) 1377.
53 M. Březina, J. Koryta and M. Musilová, Collect. Czech. Chem. Commun., 33 (1968) 3397.
54 T.G. Clarke, N.A. Hamspon, J.B. Lee, J.R. Morley and B. Scanlon, Can. J. Chem., 46 (1968) 3437.
55 T.G. Clarke, N.A. Hampson, J.B. Lee, J.R. Morley and B. Scanlon, Ber. Bunsenges, Phys. Chem., 73 (1969) 279.
56 R.D. Giles and J.A. Harrison, J. Electroanal. Chem., 27 (1970) 161.
57 R. Memming, F. Möllers and G. Neumann, J. Electrochem. Soc., 117 (1970) 451.
58 B. Miller, J. Electrochem. Soc., 117 (1970) 491.
59 B.V. Tilak, R.S. Perkins, H.A. Kozlowska and B.E. Conway, Electrochim. Acta, 17 (1972) 1447.
60 R.S. Perkins, B.V. Tilak, B.E. Conway and H.A. Kozlowska, Electrochim. Acta, 17 (1972) 1471.
61 T.P. Hoar and C.K. Dyer, Electrochim. Acta, 17 (1972) 1563.
62 T. Yoshimura and M. Yamashita, Doshisha Daigaku Rikogaku Kenkyu Hokoku, 13 (1973) 204.
63 N.A. Hampson, K.I. MacDonald and J.B. Lee, J. Electroanal. Chem., 45 (1973) 149.
64 J. Ambrose and R.G. Barradas, Electrochim. Acta, 19 (1974) 781.
65 H. Sasaki and S. Toshima, Electrochim. Acta, 20 (1975) 201.
66 A. Kunugi, S. Miyoshi and S. Nagaura, Bull. Chem. Soc. Jap., 51 (1978) 700.
67 J.M.M. Droog, P.T. Alderliesten and G.A. Bootsma, J. Electroanal. Chem., 99 (1979) 173.
68 J.M.M. Droog, J. Electroanal. Chem., to be published.
69 G.L. Vidovich, D.I. Leikis and B.N. Kabanov, Dokl. Akad. Nauk S.S.S.R., 142 (1962) 5.
70 A.I. Oshe, Sov. Electrochem., 4 (1968) 1093.
71 M. Fleischmann, D.J. Lax and H.R. Thirsk, Trans. Faraday Soc., 64 (1968) 3128.
72 M. Fleischmann, D.J. Lax and H.R. Thirsk, Trans. Faraday Soc., 64 (1968) 3137.
73 L.I. Lyamina, N.I. Tarasova and K.M. Gorbunova, Tezisy Dokl.-Soveshch. Kinet. Mekh. Khim. Reakts. Tverd. Tele, 3 (1977) 52.
74 A. Vashkyalis and O. Demontaite, Elektrokhimiya, 14 (1978) 1213.

75 R.C. Weast (Ed.), Handbook of Chemistry and Physics, 55th ed., C.R.C. Press, Cleveland, 1974.
76 A.N. Kolmogoroff, Bull. Acad. Sci., U.R.S.S. (Cl. Sci. Math. Nat.), 3 (1937) 355.
77 M. Avrami, J. Chem. Phys., 7 (1939) 1103.
78 M. Avrami, J. Chem. Phys., 8 (1940) 212.
79 M. Avrami, J. Chem. Phys., 9 (1941) 177.
80 U.R. Evans, Trans. Faraday Soc., 41 (1945) 365.
81 B.V. Erofeev, Dokl. Akad. Nauk S.S.S.R., 52 (1946) 515.
82 V.B. Fedorov, D.K. Khakimova, M.Kh. Shorshorov, N.N. Shipikov and M.A. Avdeenko, Dokl. Akad Nauk. S.S.S.R., 222 (1975) 489.
83 K.R. Brownstein and C.E. Tarr, Chem. Phys. Lett., 49 (1977) 80.